

Boosting Room-Temperature Li^+ Conductivity via strain in solid electrolytes for Lithium-ion Batteries

Rodolpho Mouta

*Departamento de Física, Universidade Federal do Maranhão,
São Luis, Maranhão, 65080-805, Brazil*

Carlos William de Araujo Paschoal

*Departamento de Física, Universidade Federal do Ceará,
Fortaleza, Ceará, 60455-554, Brazil**

(Dated: February 19, 2022)

Abstract

Room-temperature (RT) conductivity of most candidates for solid electrolytes of miniaturized lithium-ion batteries is still 1-2 orders of magnitude below commercial requirements, therefore several approaches are being pursued aiming the enhancement of such values. In this letter, we report for the first time direct theoretical evidence that epitaxial strain can be an efficient tool to reach this goal.

PACS numbers: 95.55.Sh, 93.90.+y, 13.15.+g

Significant effort is now being devoted to developing solid materials that can replace Li-based liquid electrolytes currently used in lithium-ion batteries (LIBs), since Li-based liquid electrolytes are flammable, toxic, incompatible with the highest specific energy anode (lithium metal), and pose a limit to miniaturization.[1–4] However, at room-temperature (RT), Li^+ conductivity in the best solid electrolytes (≤ 25 mS/cm) is still 1-2 orders of magnitude below that in liquid counterparts (> 100 mS/cm).[5–8] Several attempts are being performed to solve this issue, including search and design of new materials as well as the properties tailoring of well-established materials using non-stoichiometry, doping, chemical substitutions and refined synthesis techniques. [3, 5–10] An approach that has been proven particularly efficient to improve O^{2-} transport in electrolytes of miniaturized all-solid-state fuel cells is the use of epitaxial strain obtained by depositing a thin-film on a substrate with a mismatching lattice parameter.[11–17] Recently, Tealdi et al [18] also used this approach to predict a one order of magnitude enhancement at 500 K for cathodes of Li- and Na-ion batteries, with an even larger enhancement being expected at room temperature. Notwithstanding, no analogue strain-induced enhancement has been reported so far in Li^+ -conducting candidates for solid electrolytes in miniaturized LIBs. [19, 20]

In this Letter, we show clearly a significant Li^+ conductivity enhancement (by orders of magnitude) induced by strain in a solid electrolyte, opening a new window for ionic transport improvement in such materials, aiming their use in miniaturized LIBs. Our result was obtained by calculating an analytical expression for the relative change that strain induces in Li_3OCl , a prototype member of a promising family of potential solid electrolytes for LIBs that has received increasing attention in the past few years: the so-called Lithium-Rich Anti-Perovskites (LiRAPs). [3, 4, 6, 10, 21–35] Such expression was obtained in terms of the Gibbs energy barriers for Li^+ migration, which were evaluated numerically by computational modeling.

Analytical model and numeric evaluation - The analytical expression for ionic conductivity σ was calculated according to the hopping model, which can always be used as long as one knows the crystal structure, all relevant charge carriers, their concentration and the possible migration paths. Thus, considering the conductivity as [36]

$$\sigma = \sum_i n_i |q_i| \mu_i, \quad (1)$$

we used statistical thermodynamics to calculate the concentration n_i of each one of the

charge carriers, whose charges are q_i , lying at distinct positions i inside the unit cell at a temperature T . The mobility μ_i of each of them is given by [36, 37]

$$\mu_i = \frac{|q_i| \nu \beta}{2k_B T} \sum_j (\rho_{i \rightarrow j})^2 \exp\left(-G_{i \rightarrow j}^{(m)}/k_B T\right), \quad (2)$$

in which we take into account all neighboring positions j to which the carrier can migrate, these lying at distances (projected at the external applied electric field direction) $|\rho_{i \rightarrow j}|$ from position i . The above expression for mobility is based on the fact that between positions i and j there is a Gibbs energy migration barrier $G_{i \rightarrow j}^{(m)}$ that the charge carrier tries to hop with attempt frequency ν , having probability of success at each try given by the exponential term. We highlight that this model has been widely and successfully used both by theoreticians and experimentalists to replicate, model and explain the ionic transport in crystalline materials. [36, 38–44]

For a unstrained cubic (anti-)perovskite-structured ABX_3 crystal having vacancies of X ion as charge carriers, the ionic conductivity can be written as [45]

$$\sigma_o = \frac{2}{3} \nu \beta n (a_o |q_X|)^2 \exp\left(-\beta G_o^{(m)}\right), \quad (3)$$

in which $\beta = (k_B T)^{-1}$ with k_B being the Boltzmann constant, a_o is the unstrained lattice parameter, $G_o^{(m)}$ is the migration Gibbs energy from one vertex of the BX_6 octahedron to another and n is the amount of X vacancies per unit volume. In doped or non-stoichiometric crystals this amount usually is strain- and temperature-independent, being defined by the doping or non-stoichiometry degree, as long as the concentration of thermally activated charge carriers can be neglected, as usually happens at RT. This is, for example, the case of Li_3OCl antiperovskite, in which the number of thermally activated charge carriers per unit formula is $\sim 10^{-7}$ [25], while the corresponding values due to doping and non-stoichiometry are $> 5 \times 10^{-3}$ [21, 26] and $\sim 10^{-2}$ [3], respectively.

However, if a biaxial stress is applied in the [100] and [010] directions, cubic symmetry is broken and Eq. (3) no longer holds. Considering that no octahedral tilt occurs and all ions remain in their original fractional coordinates relative to the lattice parameters, the basal plane contraction (compressive stress) or expansion (tensile stress) leads to a tetragonal structure. Thus, the X ions in planes (001) (in apical positions relative to the BX_6 octahedra) and X ions in planes (002) (in equatorial positions relative to the octahedra) are no longer equivalent by symmetry. This implies that apical and equatorial vacancies will

have distinct formation Gibbs energies $G_{ap}^{(\nu)}$ and $G_{eq}^{(\nu)}$, so that ion X vacancies will tend to concentrate in planes with lowest Gibbs energy. Also, there are now three distinct vacancy migration paths: (i) equatorial-to-equatorial, (ii) equatorial-to-apical, and (iii) apical-to-equatorial, with respective migration Gibbs energies $G_{eq\rightarrow eq}^{(m)}$, $G_{eq\rightarrow ap}^{(m)}$ and $G_{ap\rightarrow eq}^{(m)}$ (apical-to-apical migration barrier is always large, with negligible contribution to mobility).

This leads to distinction between lateral (i.e., in the same plane of applied stress) and perpendicular (to the plane of applied stress) conductivities. We noticed strain was always detrimental to perpendicular transport in Li_3OCl (and apparently for perovskites in general), so here we focus on the lateral conductivity only, which on this case is

$$\sigma = \nu\beta n (a |q_X|)^2 e^{-\beta G_{eq\rightarrow eq}^{(m)}} \left[\frac{1 + e^{-\beta(G_{eq\rightarrow ap}^{(m)} - G_{eq\rightarrow eq}^{(m)})}}{2 + e^{-\beta(G_{ap}^{(\nu)} - G_{eq}^{(\nu)})}} \right], \quad (4)$$

where a is the strained lattice parameter parallel to any one of the two equivalent directions of applied stress. Thus the ratio between lateral ionic conductivities of the strained and the unstrained crystal is

$$\frac{\sigma}{\sigma_o} = \frac{3}{2} \left(\frac{a}{a_o} \right)^2 e^{\beta(G_o^{(m)} - G_{eq\rightarrow eq}^{(m)})} \left[\frac{1 + e^{-\beta(G_{eq\rightarrow ap}^{(m)} - G_{eq\rightarrow eq}^{(m)})}}{2 + e^{-\beta(G_{ap}^{(\nu)} - G_{eq}^{(\nu)})}} \right] \quad (5)$$

Therefore, to determine the relative increase (or decrease) in Li_3OCl 's Li^+ conductivity as a function of biaxial strain, we just need to know how the lattice parameter, as well as Gibbs energies of formation and migration of Li^+ vacancies, depend on strain. Classical atomistic modelling is a powerful and reliable tool to access defect energetics in energy materials (including LIB materials) [18, 25, 35, 46–50] and to estimate the effect of strain on ionic transport.[13, 18, 51–53] Thus, we performed quasi-static calculations based on pairwise interionic potentials using the GULP code [54–56] to obtain the lattice parameter and Li^+ vacancies formation and migration Gibbs energies required in Eq. (5) as a function of tensile biaxial strain for Li_3OCl . We adopted a robust, already validated parameterization previously derived by our group,[25, 31, 35] since the resulting force field has the unusual advantage of allowing the straightforward calculation of Gibbs energies, instead of enthalpies. This is important because neglecting entropy contributions may lead to uncertainties as large as one order of magnitude.[13] All parameters in Eq. (5) were calculated at 300 K, since this is the ideal LIB operation temperature. We also point out that in the range of biaxial strains investigated (0-6%), the only structural change observed in our calculations was a

simple tetragonal distortion, without any octahedral tilts, so that all assumptions leading to Eq. (5) were satisfied.

Ionic conductivity boost and implications for epitaxial films - The calculated relative enhancement in lateral Li^+ conductivity as a function of tensile biaxial strain, as shown in Fig. 1, indicates that a huge conductivity increase, nearly with exponential behavior, can be achieved with relatively low strains, with the ionic conductivity increasing by over one order of magnitude at 2% and reaching a two orders of magnitude enhancement already at 3.3%. Considering that the RT Li^+ conductivities of Li_3OCl -based polycrystals ($10^{-4} - 10^{-3}$ S/cm) [3, 5, 21, 27] are among the highest ones reported for crystalline materials, the possibility of enhancing such values by even 1-2 orders of magnitude is remarkable, since this may improve significantly this electrolyte performance in miniaturized LIBs. We stress that this is the first clear evidence of strain-induced enhancement in ionic transport of a Li^+ -conducting solid electrolyte [19]. For completeness sake, we also investigated influence of tensile biaxial strain over perpendicular conductivity (not shown here), but it was found to be detrimental. Also, further calculations for compressive biaxial strains revealed that these are detrimental not only to perpendicular, but also to lateral transport. A detailed investigation of Li_3OCl 's ionic conductivity dependence on different strain states is beyond the scope of this Letter and will be published elsewhere.

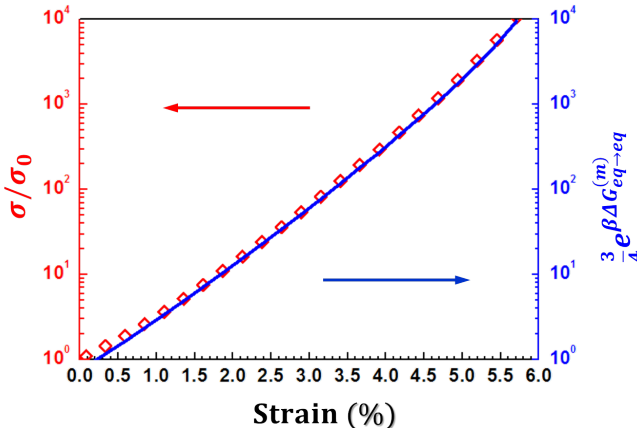


FIG. 1. (Color online) Ratio between lateral conductivities of strained and unstrained Li_3OCl for a tensile biaxial strain in the directions $[100]$ and $[010]$, calculated from both the full expression, Eq. (5) (red diamonds), and the simple approximation given by Eq. (9) (blue line).

These findings have important implications for Li_3OCl thin films use as solid electrolytes

in miniaturized LIBs. The commonest way to obtain a tensile strain is by depositing an epitaxial film on a substrate whose lattice parameter is larger than that of the ionic conductor. For Li_3OCl , a commercially available substrate which implies a tensile strain around 2% is $\text{K}(\text{Ta}_{1-x}\text{Nb}_x)\text{O}_3$ (KTN), whose lattice parameter ranges from 3.989 to 4.000 Å depending on Nb concentration. Commonly used substrates as SrTiO_3 , LaAlO_3 and YAlO_3 have lattice parameter lower than Li_3OCl and should not imply in a conductivity enhancement if Li_3OCl grows in [001] direction on these substrates. Also, substrates with very larger lattice parameter which are almost a_o multiples can be used, but in this case the epitaxial deposition is difficult. Finally, a non-strained thick film with the desired lattice parameter can be grown in a conventional substrate as an intermediated layer to drive a tensile strain in Li_3OCl . For example, Li_3OBr ($a \sim 4.045$ Å) can be used as such intermediate layer, delivering a tensile strain of *ca.* 3.5%.

Furthermore, the electrodes should be placed on the sides of the film (see Fig. 2), instead of sandwiching it from below and above, as it is usually performed for perovskites' epitaxial growth by sputtering or pulsed laser deposition (PLD), when a conductor perovskite layer, as SrRuO_3 , is first deposited. It is necessary to use lateral electrodes so that lateral, instead of perpendicular conductivity, is obtained. This setup has already been successfully employed to observe a two orders of magnitude enhancement in lateral ionic conductivity at 573 K due to tensile biaxial strain in a yttria-stabilized zirconia (YSZ) thin film deposited on SrTiO_3 (STO) substrate. [12] Another possible setup is to place both electrodes on top, instead of on the sides. This is similar to the setup employed by García-Barriocanal *et al.* [11] to observe an eight orders of magnitude enhancement in lateral conductivity of YSZ near RT (357 K) in YSZ/STO heterostructures, which has been partially attributed to strain.[13, 57] However, it has been argued that this later setup may lead to “enormous electrode resistance” [58] due to the small contact between the electrodes and the system under study, so that the one presented in Fig. 2 may be more suitable.

Exponential dependence of ionic conductivity on strain - Along with the conductivity enhancement in itself, its simple exponential dependence on strain is also very interesting from a physical point of view, once it is not directly obvious from Eq. (5). Therefore, we further investigated this dependence, getting helpful physical insights along the way, as shown next. For tensile strains, the calculated Gibbs energy of formation of equatorial

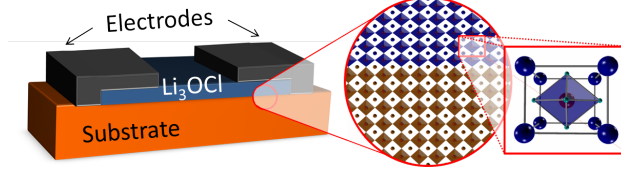


FIG. 2. (Color online) Apparatus suggested for future experimental probe of lateral conductivity enhancement in a Li_3OCl thin film, induced by epitaxial strain due to lattice parameter mismatch between the film and substrate. The inset shows the resulting tensile strain in the Li_3OCl 's unit cell.

vacancies was lower than of apical vacancies, as can be seen in Fig. 3(a), so that

$$G_{ap}^{(\nu)} - G_{eq}^{(\nu)} > 0. \quad (6)$$

Also, according to Fig. 3(b), the Gibbs energy barrier for equatorial-to-equatorial migration is lower than the unstrained counterpart. Thus, for non-zero strain,

$$\Delta G_{eq \rightarrow eq}^{(m)} \equiv G_0^{(m)} - G_{eq \rightarrow eq}^{(m)} > 0. \quad (7)$$

As also shown in Fig. 3(a), the equatorial-to-apical migration barrier is higher than the unstrained one, since Gibbs energy of formation of an equatorial vacancy decreases faster with strain than the saddle point Gibbs energy does. For example, for 5%, the contours show that Gibbs energy of formation of an equatorial vacancy is reduced by more than 0.2 eV, while the saddle point Gibbs energy is reduced by less than 0.2 eV. Accordingly, also for non-zero strain,

$$G_{eq \rightarrow ap}^{(m)} - G_{eq \rightarrow eq}^{(m)} > 0. \quad (8)$$

Our calculations showed all these differences grow almost linearly when strain increases, in a rate high enough for the corresponding exponentials of the differences present in Eq. (6) and in Eq. (8) to become negligible for strains greater than 1%. In this case, Eq. (5) reduces simply to

$$\frac{\sigma}{\sigma_o} \approx \frac{3}{4} e^{\beta \Delta G_{eq \rightarrow eq}^{(m)}}, \quad (9)$$

since the variation in the lattice parameter is small compared to the exponential above. Therefore, for strains greater than 1%, Eq. (9) can provide a great estimate of relative increase in Li_3OCl 's lateral ionic conductivity compared to the full expression, as observed in Fig.1. Notice Eq.(9) directly explains the nearly exponential behavior obtained, since

the dependence of equatorial-to-equatorial Gibbs energy barriers on strain was found to be almost linear.

Despite this exponential impact of strain over conductivity, it is important to observe that strain may not be so helpful to increase conduction at high temperatures, once the relative increase in conductivity has exponential dependence also on the inverse of temperature. This is consistent with molecular dynamics calculations at very high temperatures on LaGaO_3 , where the increase in lateral diffusion was small, yet exponential on strain.[53] However, while performance at high/intermediate temperatures is critical for a potential solid oxide fuel cell electrolyte such as LaGaO_3 , the ideal operation temperature of a LIB is RT, so the fact that conductivity enhancement at higher temperatures may be small is not a problem for Li_3OCl . Besides, its conductivity already increases rapidly to very high values at superior temperatures, due to its low activation enthalpy.

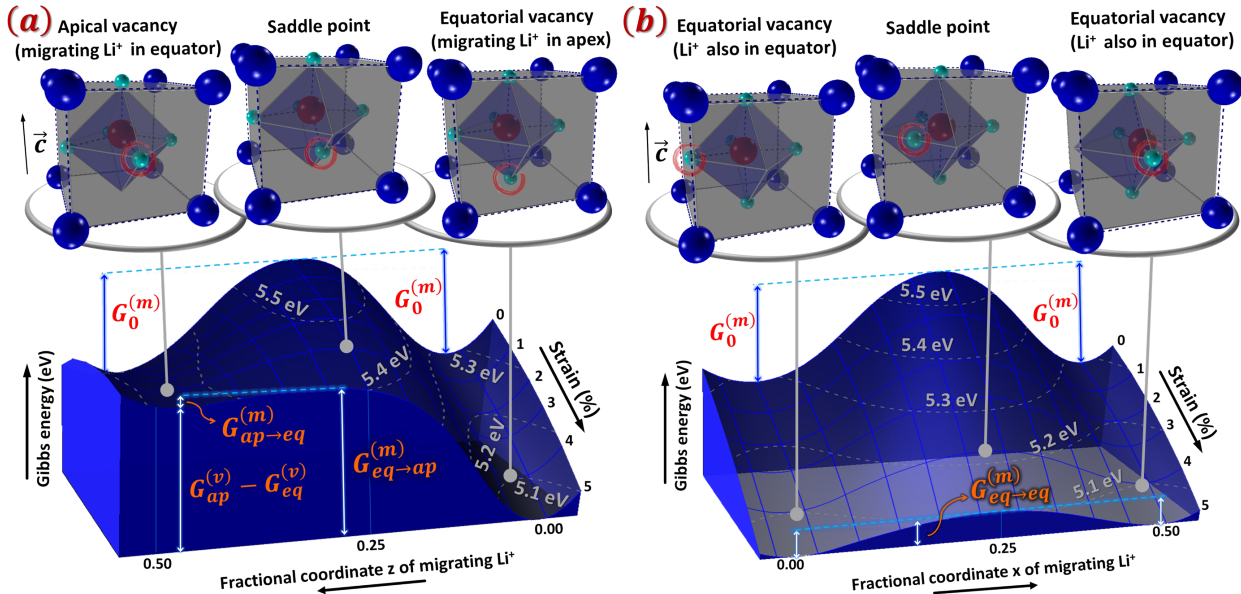


FIG. 3. (Color online) Gibbs energy barrier profiles as a function of strain for (a) equatorial-to-apical and (b) equatorial-to-equatorial migration, obtained from atomistic modelling. The grey dashed contours provide reference to numeric values of Gibbs energy, while blue filled lines evidence the barrier profile for a fixed strain value. Superior insets show snapshots of the relaxed structure around the migrating Li^+ vacancy, with Li^+ , O^{2-} and Cl^- colored cyan, red and blue, respectively, and blue dashed lined connecting ions to help visualizing structural distortions in relation to the initial structure (i.e., undistorted and without vacancies).

Microscopic insights - Now we turn our attention to the terms present in Eq. (5), but missing in Eq. (9), since this comparison leads to further insights about the the preferential migration path and the distribution of vacancies between apical and equatorial sites. First, we observe that the main feature contributing for the strain-induced enhancement in Li^+ conduction is the reduction of equatorial-to-equatorial barrier, without any significant influence from the other two. This can be explained by degeneracy breaking of vacancy formation Gibbs energy, which splits into two values, one for each plane. On one hand, this split makes the (001) planes energetically unfavorable for vacancies, so that too few vacancies (2% for strains as low as 1%) are in apical positions for the apical-to-equatorial hopping contribution to be relevant. On the other hand, it increases Gibbs energy of equatorial-to-apical hopping, once the ground state for migration lowers (more than the saddle point does; see Fig. 3(a)), limiting significantly the amount of hops by this route. Therefore, lateral conduction happens almost exclusively in (002) planes; accordingly, only the migration barrier in these planes are relevant for strains $>\sim 1\%$.

Second, at first sight, the transport in (002) planes is not strongly influenced by the drastic increase of equatorial vacancy concentration, once Eq. (9) has no dependence on the relative formation Gibbs energies. This is intriguing, since the conductivity is linearly proportional to the charge carriers concentration in each plane and should be very sensitive to them, as described by Eq. (1). However, a closer look in the statistical distribution of vacancies over the two planes as a function of strain reveals that the percent of equatorial vacancies is already $\sim 98\%$ for strains as low as 1%, being $>99\%$ when strain is 1.4%, hence with only minor increments. Therefore, for strains greater than 1%, the concentration of equatorial vacancies saturates, reaching a practically constant value. Accordingly, its contribution to Eq. (9) is also a constant value, embedded in the pre-exponential term.

Further applicability - We highlight that despite the considerations that led to Eq. (9) did not take into account octahedral tilts, apparently this exponential dependence is also valid when tilts are present, as in the case of perovskite LaGaO_3 , for example. It is easy to verify that our very simple Eq. (9) is able to reproduce with remarkable accuracy the relative increase in LaGaO_3 's lateral transport as obtained by Tealdi and Mustarelli using molecular dynamics, [53] an approach that is much more computationally expensive and time consuming than static defect calculations.

We infer that the applicability of Eq. (9) to (anti)perovskite-structured materials is

primarily associated to the reduction in equatorial-to-equatorial migration barrier and to the strain-induced split of vacancy formation Gibbs energy, and hence reallocation of all vacancies to equatorial positions already for small strains, instead of other structural features such as octahedral tilts. More interestingly, such exponential dependence seems to hold even for structures other than perovskite, such as fluorite, as shown by De Souza *et al.* for ceria.[13] Therefore, the exponential dependence appears to have a somewhat general validity and turns out to be a simple way to estimate the effect of biaxial strain on parallel conductivity from theoretical values of Gibbs energy barriers or enthalpy barriers, as an approximation to Gibbs energy when migration entropy does not vary significantly with strain.

Conclusions and perspectives - Summarizing, in this Letter we showed that strain is a powerful tool to boost RT Li^+ conductivity in thin-film solid electrolytes for miniaturized LIBs. We exemplified this by calculating the relative enhancement in ionic conductivity that biaxial tensile strain can induce in a promising solid electrolyte, Li_3OCl , in which a two orders of magnitude increase was predicted for a 3.3% strain. We also provided practical suggestions on experimental setup and strategies to observe this effect, which may lead to the larger Li^+ conductivity ever reported in a solid electrolyte. We established an analytical expression for the strain-induced enhancement valid for vacancy migration between octahedra vertices in perovskite-structured solids in general, so it can also be used to probe the same effect in a wide range of other O^{2-} , Li^+ and Na^+ conductors candidates for solid electrolytes in fuel cells or alkali-metal-ion batteries, such as perovskite oxides, [53] other LiRAPs and also NaRAPs (Na-Rich Anti-Perovskites) [59, 60]. Finally, the approach used here can also be scaled for more complex structures other than perovskite.

We thank J. Gale for permitting us use the GULP code and the Brazilian funding agencies CAPES and CNPq for partially supporting this research. We are also grateful to E. F. V. Carvalho and E. N. Silva for computational facilities, and C. A. C. Feitosa for enlightening discussions.

* paschoal.william@fisica.ufc.br

[1] Eliana Quartarone and Piercarlo Mustarelli. Electrolytes for solid-state lithium rechargeable

- batteries: recent advances and perspectives. *Chemical Society reviews*, 40(5):2525–2540, 2011.
- [2] Nam-Soon Choi, Zonghai Chen, Stefan A Freunberger, Xiulei Ji, Yang-Kook Sun, Khalil Amine, Gleb Yushin, Linda F Nazar, Jaephil Cho, and Peter G Bruce. Challenges facing lithium batteries and electrical double-layer capacitors. *Angewandte Chemie (International ed. in English)*, 51(40):9994–10024, oct 2012.
- [3] Yusheng Zhao and Luke L Daemen. Superionic conductivity in lithium-rich anti-perovskites. *Journal of the American Chemical Society*, 134(36):15042–7, sep 2012.
- [4] Xujie Lü, John W. Howard, Aiping Chen, Jinlong Zhu, Shuai Li, Gang Wu, Paul Dowden, Hongwu Xu, Yusheng Zhao, and Quanxi Jia. Antiperovskite Li_3OCl Superionic Conductor Films for Solid-State Li-Ion Batteries. *Advanced Science*, pages n/a–n/a, feb 2016.
- [5] Noriaki Kamaya, Kenji Homma, Yuichiro Yamakawa, Masaaki Hirayama, Ryoji Kanno, Masao Yonemura, Takashi Kamiyama, Yuki Kato, Shigenori Hama, Koji Kawamoto, and Akio Mitsui. A lithium superionic conductor. *Nature materials*, 10(9):682–686, 2011.
- [6] M. Helena Braga, Andrew J. Murchison, Jorge A. Ferreira, Preetam Singh, and John B. Goodenough. Glass-amorphous alkali-ion solid electrolytes and their performance in symmetrical cells. *Energy Environ. Sci.*, 9(3):948–954, 2016.
- [7] Yoshikatsu Seino, Tsuyoshi Ota, Kazunori Takada, Akitoshi Hayashi, and Masahiro Tatsumisago. A sulphide lithium super ion conductor is superior to liquid ion conductors for use in rechargeable batteries. *Energy Environ. Sci.*, 7(2):627–631, 2014.
- [8] Yuxin Tang, Yanyan Zhang, Wenlong Li, Bing Ma, and Xiaodong Chen. Rational material design for ultrafast rechargeable lithium-ion batteries. *Chem. Soc. Rev.*, 44(17):5926–5940, 2015.
- [9] Gayatri Sahu, Ezhiylmurugan Rangasamy, Juchuan Li, Yan Chen, Ke An, Nancy Dudney, and Chengdu Liang. A high-conduction Ge substituted Li_3AsS_4 solid electrolyte with exceptional low activation energy. *Journal of Materials Chemistry A*, 2(27):10396, 2014.
- [10] Zhi Deng, Balachandran Radhakrishnan, and Shyue Ping Ong. Rational Composition Optimization of the Lithium-Rich $\text{Li}_3\text{OCl}_{1-x}\text{Br}_x$ Anti-Perovskite Superionic Conductors. *Chemistry of Materials*, 27(10):3749–3755, may 2015.
- [11] J. Garcia-Barriocanal, A. Rivera-Calzada, M. Varela, Z. Sefrioui, E. Iborra, C. Leon, S. J. Pennycook, and J. Santamaria. Colossal Ionic Conductivity at Interfaces of Epitaxial $\text{ZrO}_2\text{:Y}_2\text{O}_3/\text{SrTiO}_3$ Heterostructures. *Science*, 321(5889):676–680, aug 2008.

- [12] Michael Sillassen, Per Eklund, Nini Pryds, Erik Johnson, Ulf Helmersson, and Jørgen Bøttiger. Low-Temperature Superionic Conductivity in Strained Yttria-Stabilized Zirconia. *Advanced Functional Materials*, 20(13):2071–2076, may 2010.
- [13] Roger A. De Souza, Amr Ramadan, and Stefanie Hörner. Modifying the barriers for oxygen-vacancy migration in fluorite-structured CeO₂ electrolytes through strain: a computer simulation study. *Energy Environ. Sci.*, 5(1):5445–5453, 2012.
- [14] Markus Kubicek, Zhuhua Cai, Wen Ma, Bilge Yildiz, Herbert Hutter, and Jürgen Fleig. Tensile Lattice Strain Accelerates Oxygen Surface Exchange and Diffusion in La_{1-x}Sr_xCoO_{3-δ} Thin Films. *ACS Nano*, 7(4):3276–3286, apr 2013.
- [15] Bilge Yildiz. Stretching the energy landscape of oxides Effects on electrocatalysis and diffusion. *MRS Bulletin*, 39(02):147–156, feb 2014.
- [16] Anuj Goyal, Simon R. Phillpot, Gopinath Subramanian, David A. Andersson, Chris R. Stanek, and Blas P. Uberuaga. Impact of homogeneous strain on uranium vacancy diffusion in uranium dioxide. *Physical Review B*, 91(9):094103, mar 2015.
- [17] Shinbuhm Lee, Wenrui Zhang, Fauzia Khatkhatay, Quanxi Jia, Haiyan Wang, and Judith L. MacManus-Driscoll. Strain Tuning and Strong Enhancement of Ionic Conductivity in SrZrO₃-RE₂O₃ (RE = Sm, Eu, Gd, Dy, and Er) Nanocomposite Films. *Advanced Functional Materials*, 25(27):4328–4333, jul 2015.
- [18] Cristina Tealdi, Jennifer Heath, and M. Saiful Islam. Feeling the strain: enhancing ionic transport in olivine phosphate cathodes for Li- and Na-ion batteries through strain effects. *J. Mater. Chem. A*, 2016.
- [19] John Christopher Bachman, Sokseiha Muy, Alexis Grimaud, Hao-Hsun Chang, Nir Pour, Simon F. Lux, Odysseas Paschos, Filippo Maglia, Saskia Lupart, Peter Lamp, Livia Giordano, and Yang Shao-Horn. Inorganic Solid-State Electrolytes for Lithium Batteries: Mechanisms and Properties Governing Ion Conduction. *Chemical Reviews*, 116(1):140–162, jan 2016.
- [20] Jie Wei, Daisuke Ogawa, Tomoteru Fukumura, Yasushi Hirose, and Tetsuya Hasegawa. Epitaxial Strain-Controlled Ionic Conductivity in Li-Ion Solid Electrolyte Li_{0.33}La_{0.56}TiO₃ Thin Films. *Crystal Growth & Design*, 15(5):2187–2191, may 2015.
- [21] M. H. Braga, J. A. Ferreira, V. Stockhausen, J. E. Oliveira, and A. El-Azab. Novel Li₃ClO based glasses with superionic properties for lithium batteries. *Journal of Materials Chemistry A*, 2(15):5470, 2014.

- [22] Olaf Reckeweg, Björn Blaschkowski, and Thomas Schleid. Li_5OCl_3 and Li_3OCl : Two Remarkably Different Lithium Oxide Chlorides. *Zeitschrift für anorganische und allgemeine Chemie*, 638(12-13):2081–2086, oct 2012.
- [23] Yi Zhang, Yusheng Zhao, and Changfeng Chen. Ab initio study of the stabilities of and mechanism of superionic transport in lithium-rich antiperovskites. *Physical Review B*, 87(13):134303, apr 2013.
- [24] Alexandra Emly, Emmanouil Kioupakis, and Anton Van der Ven. Phase Stability and Transport Mechanisms in Antiperovskite Li_3OCl and Li_3OBr Superionic Conductors. *Chemistry of Materials*, 25(23):4663–4670, dec 2013.
- [25] Rodolpho Mouta, Maria Águida B Melo, Eduardo M Diniz, and Carlos William A Paschoal. Concentration of Charge Carriers, Migration, and Stability in Li_3OCl Solid Electrolytes. *Chemistry of Materials*, 26(24):7137–7144, nov 2014.
- [26] Jianzhong Zhang, Jiantao Han, Jinlong Zhu, Zhijun Lin, Maria H. Braga, Luke L. Daemen, Liping Wang, and Yusheng Zhao. High pressure-high temperature synthesis of lithium-rich $\text{Li}_3\text{O}(\text{Cl},\text{Br})$ and $\text{Li}_{3-x}\text{Ca}_{x/2}\text{OCl}$ anti-perovskite halides. *Inorganic Chemistry Communications*, 48:140–143, oct 2014.
- [27] Xujie Lü, Gang Wu, John W Howard, Aiping Chen, Yusheng Zhao, Luke L Daemen, and Quanxi Jia. Li-rich anti-perovskite Li_3OCl films with enhanced ionic conductivity. *Chemical communications (Cambridge, England)*, 50(78):11520–2, oct 2014.
- [28] D. J. Schroeder, A. A. Hubaud, and J. T. Vaughey. Stability of the solid electrolyte Li_3OBr to common battery solvents. *Materials Research Bulletin*, 49:614–617, jan 2014.
- [29] J. Zhang, J. Zhu, L. Wang, and Y. Zhao. A new lithium-rich anti-spinel in LiOBr system. *Chem. Commun.*, 51(47):9666–9669, 2015.
- [30] Min-Hua Chen, Alexandra Emly, and Anton Van der Ven. Anharmonicity and phase stability of antiperovskite Li_3OCl . *Physical Review B*, 91(21):214306, jun 2015.
- [31] Ziheng Lu, Chi Chen, Zarah Medina Baiyee, Xin Chen, Chunming Niu, and Francesco Ciucci. Defect chemistry and lithium transport in Li_3OCl anti-perovskite superionic conductor. *Phys. Chem. Chem. Phys.*, 2015.
- [32] Shuai Li, Jinlong Zhu, Yonggang Wang, John W. Howard, Xujie Lü, Yutao Li, Ravhi S. Kumar, Liping Wang, Luke L. Daemen, and Yusheng Zhao. Reaction mechanism studies towards effective fabrication of lithium-rich anti-perovskites Li_3OX ($\text{X}=\text{Cl}, \text{Br}$). *Solid State*

- Ionics*, 284:14–19, jan 2016.
- [33] Zhi Deng, Zhenbin Wang, Iek-Heng Chu, Jian Luo, and Shyue Ping Ong. Elastic Properties of Alkali Superionic Conductor Electrolytes from First Principles Calculations. *Journal of The Electrochemical Society*, 163(2):A67–A74, nov 2016.
- [34] Jian Gao, Yu-Sheng Zhao, Si-Qi Shi, and Hong Li. Lithium-ion transport in inorganic solid state electrolyte. *Chinese Physics B*, 25(1):018211, jan 2016.
- [35] R. Mouta, E. M. Diniz, and C. W. A. Paschoal. Li^+ interstitials as the charge carriers in superionic lithium-rich anti-perovskites. *J. Mater. Chem. A*, 4(5):1586–1590, 2016.
- [36] Sean R. Bishop, Harry L. Tuller, Melanie Kuhn, Guido Ciampi, William Higgins, and Kanai S. Shah. Kinetics of Schottky defect formation and annihilation in single crystal TlBr. *Physical Chemistry Chemical Physics*, 15(28):11926, 2013.
- [37] A B Lidiard. Electrical Conductivity II. In *Handbuch der Physik*, chapter Ionic Conductivity, pages 246–349. Springer Berlin Heidelberg, Berlin, Heidelberg, 1957.
- [38] David Lynch. Diffusion and Ionic Conductivity in Cesium Bromide and Cesium Iodide. *Physical Review*, 118(2):468–473, apr 1960.
- [39] Robert Fuller, Charles Marquardt, Michael Reilly, and John Wells. Ionic Transport in Potassium Chloride. *Physical Review*, 176(3):1036–1045, dec 1968.
- [40] Robert Fuller, Michael Reilly, Charles Marquardt, and John Wells. Electrical Conductivity of Potassium Chloride. *Physical Review Letters*, 20(13):662–664, mar 1968.
- [41] J. Aboagye and R. Friauf. Anomalous high-temperature ionic conductivity in the silver halides. *Physical Review B*, 11(4):1654–1664, feb 1975.
- [42] P. Dorenbos, S. Vrind, J. Dolfing, and H. W. den Hartog. Hopping ionic conductivity in Ce-doped SrF_2 . I. Ionic thermocurrent results. *Physical Review B*, 35(11):5766–5773, apr 1987.
- [43] A Tschöpe. Grain size-dependent electrical conductivity of polycrystalline cerium oxide I. Experiments. *Solid State Ionics*, 139(3-4):255–265, feb 2001.
- [44] C. R. A. Catlow, J. Corish and P. W. M. Jacobs. A calculation of the Frenkel defect formation energy in silver chloride. *Journal of Physics C: Solid State Physics*, 12(17): 3433, sep 1979.
- [45] A.S Nowick, Yang Du, and K.C Liang. Some factors that determine proton conductivity in nonstoichiometric complex perovskites. *Solid State Ionics*, 125(1-4):303–311, oct 1999.
- [46] Melanie Schroeder, Christopher Eames, David A Tompsett, Georg Lieser, and M Saiful Islam.

- Li_xFeF_6 ($x = 2, 3, 4$) battery materials: structural, electronic and lithium diffusion properties. *Physical chemistry chemical physics : PCCP*, 15(47):20473–9, dec 2013.
- [47] Pooja M. Panchmatia, A. Robert Armstrong, Peter G. Bruce, and M. Saiful Islam. Lithium-ion diffusion mechanisms in the battery anode material $\text{Li}_{1+x}\text{V}_{1-x}\text{O}_2$. *Phys. Chem. Chem. Phys.*, 16(39):21114–21118, jul 2014.
- [48] M Saiful Islam and Craig A J Fisher. Lithium and sodium battery cathode materials: computational insights into voltage, diffusion and nanostructural properties. *Chemical Society reviews*, 43(1):185–204, jan 2014.
- [49] John M. Clark, Christopher Eames, Marine Reynaud, Gwenaëlle Rouse, Jean-Noël Chotard, Jean-Marie Tarascon, and M. Saiful Islam. High voltage sulphate cathodes $\text{Li}_2\text{M}(\text{SO}_4)_2$ ($\text{M} = \text{Fe}, \text{Mn}, \text{Co}$): atomic-scale studies of lithium diffusion, surfaces and voltage trends. *Journal of Materials Chemistry A*, 2(20):7446, 2014.
- [50] Yue Deng, Christopher Eames, Jean-Noël Chotard, Fabien Lalère, Vincent Seznec, Steffen Emge, Oliver Pecher, Clare P. Grey, Christian Masquelier, and M. Saiful Islam. Structural and Mechanistic Insights into Fast Lithium-Ion Conduction in $\text{Li}_4\text{SiO}_4\text{-Li}_3\text{PO}_4$ Solid Electrolytes. *Journal of the American Chemical Society*, 137(28):9136–9145, jul 2015.
- [51] G. Dezanneau, J. Hermet, and B. Dupé. Effects of biaxial strain on bulk 8% yttria-stabilised zirconia ion conduction through molecular dynamics. *International Journal of Hydrogen Energy*, 37(9):8081–8086, may 2012.
- [52] M. J. D. Rushton and A. Chroneos. Impact of uniaxial strain and doping on oxygen diffusion in CeO_2 . *Scientific Reports*, 4:6068, aug 2014.
- [53] Cristina Tealdi and Piercarlo Mustarelli. Improving Oxygen Transport in Perovskite-Type LaGaO_3 Solid Electrolyte through Strain. *The Journal of Physical Chemistry C*, 118(51):29574–29582, dec 2014.
- [54] Julian D Gale. GULP: a computer program for the symmetry-adapted simulation of solids. *J. Chem. Soc. {,} Faraday Trans.*, 93(4):629–637, 1997.
- [55] Julian D Gale and Andrew L Rohl. The General Utility Lattice Program (GULP). *Molecular Simulation*, 29(5):291–341, may 2003.
- [56] Julian D Gale. GULP: Capabilities and prospects. *Zeitschrift für Kristallographie - Crystalline Materials*, 220(5-6-2005):552–554, may 2005.
- [57] Timothy J. Pennycook, Matthew J. Beck, Kalman Varga, Maria Varela, Stephen J. Penny-

- cook, and Sokrates T. Pantelides. Origin of Colossal Ionic Conductivity in Oxide Multilayers: Interface Induced Sublattice Disorder. *Physical Review Letters*, 104(11):115901, mar 2010.
- [58] X. Guo. Comment on "Colossal Ionic Conductivity at Interfaces of Epitaxial $\text{ZrO}_2\text{:Y}_2\text{O}_3\text{/SrTiO}_3$ Heterostructures". *Science*, 324(5926):465–465, apr 2009.
- [59] Yonggang Wang, Qingfei Wang, Zhenpu Liu, Zhengyang Zhou, Shuai Li, Jinlong Zhu, Ruqiang Zou, Yingxia Wang, Jianhua Lin, and Yusheng Zhao. Structural manipulation approaches towards enhanced sodium ionic conductivity in Na-rich antiperovskites. *Journal of Power Sources*, 293:735–740, oct 2015.
- [60] Yonggang Wang, Ting Wen, Changyong Park, Curtis Kenney-Benson, Michael Pravica, Wenge Yang, and Yusheng Zhao. Robust high pressure stability and negative thermal expansion in sodium-rich antiperovskites Na_3OBr and Na_4OI_2 . *Journal of Applied Physics*, 119(2):025901, jan 2016.